

## Supporting Information

### Correlating Structural Changes and Gas Evolution during the Thermal Decomposition of Charged $\text{Li}_x\text{Ni}_{0.8}\text{Co}_{0.15}\text{Al}_{0.05}\text{O}_2$ Cathode Materials

Seong-Min Bak,<sup>†,‡,¶</sup> Kyung-Wan Nam,<sup>\*,†</sup> Wonyoung Chang,<sup>‡</sup> Xiqian Yu,<sup>†</sup> Enyuan Hu,<sup>†</sup> Sooyeon Hwang,<sup>§</sup> Eric A. Stach,<sup>§</sup> Kwang-Bum Kim,<sup>¶</sup> Kyung Yoon Chung<sup>\*,‡</sup> and Xiao-Qing Yang<sup>\*,†</sup>

<sup>†</sup> Chemistry Department, Brookhaven National Laboratory, Upton, New York, 11973, United States.

<sup>‡</sup> Center for Energy Convergence, Korea Institute of Science and Technology (KIST), Seoul, 136-791, Republic of Korea.

<sup>§</sup> Center for Functional Nanomaterials, Brookhaven National Laboratory, Upton, New York, 11973, United States.

<sup>¶</sup> Department of Material Science and Engineering, Yonsei University, 134 Shinchon-dong, Seodaemoon-gu, Seoul, 120-749, Republic of Korea.

E-mail: [knam@bnl.gov](mailto:knam@bnl.gov) (K.N.); [kychung@kist.re.kr](mailto:kychung@kist.re.kr) (K.C.); [xyang@bnl.gov](mailto:xyang@bnl.gov) (X.Y.)

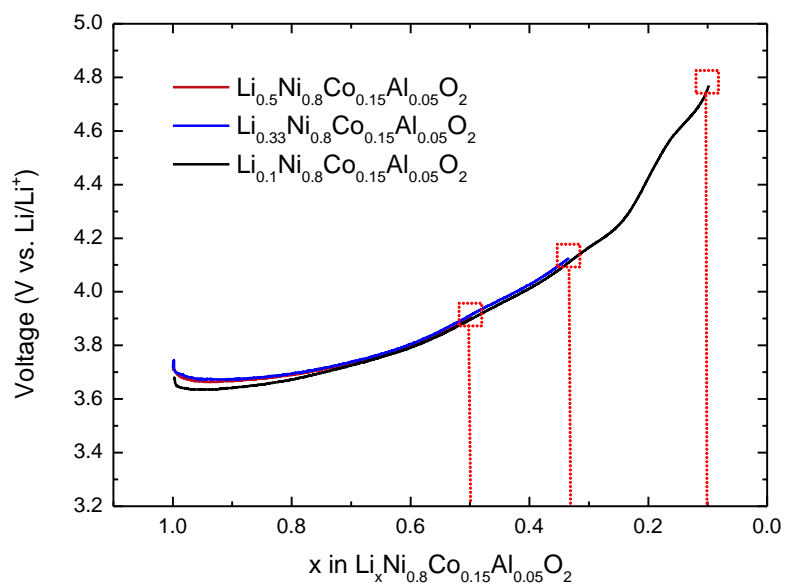


**Figure S1.** Constant current charge profiles of the  $\text{Li}_x\text{Ni}_{0.8}\text{Co}_{0.15}\text{Al}_{0.05}\text{O}_2$  ( $x=0.5, 0.33$  and  $0.1$ ) electrode with a C/18 rate.

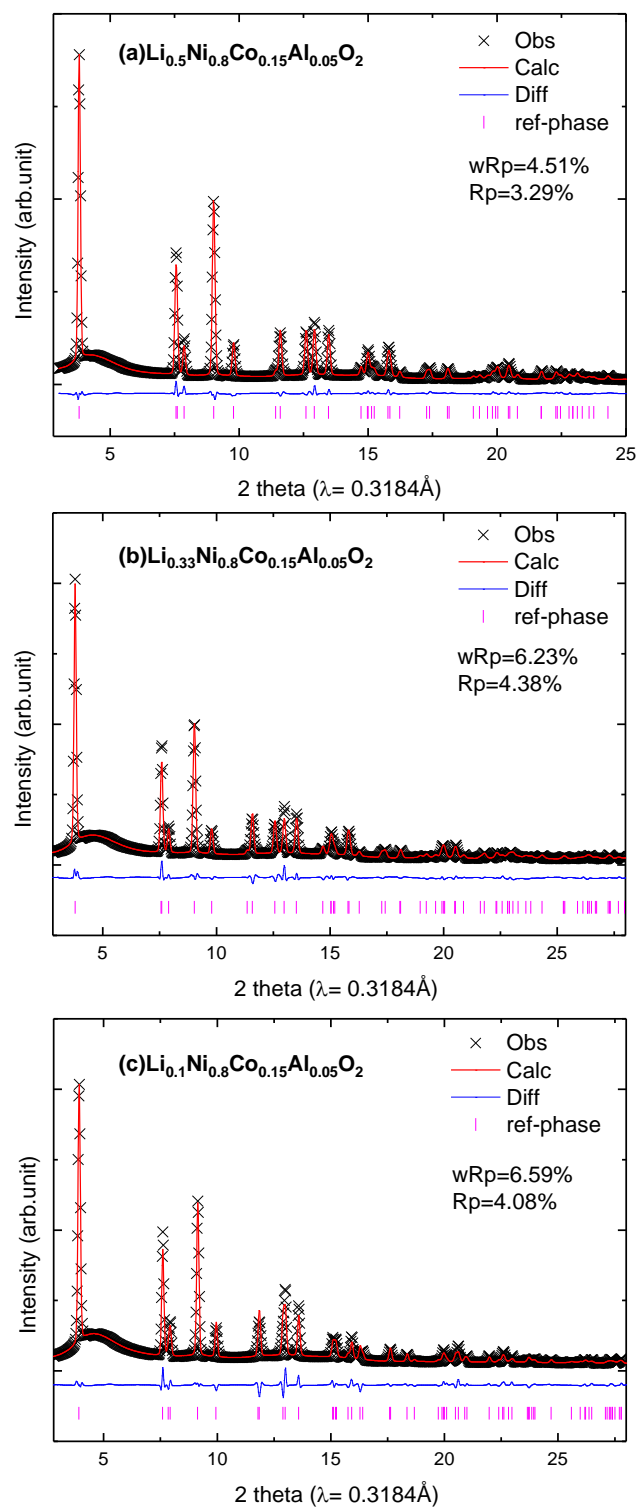


**Figure S2.** Rietveld refinement of XRD data for  $\text{Li}_x\text{Ni}_{0.8}\text{Co}_{0.15}\text{Al}_{0.05}\text{O}_2$  with (a)  $x=0.5$ , (b)  $x=0.33$ , and (c)  $x=0.1$ .

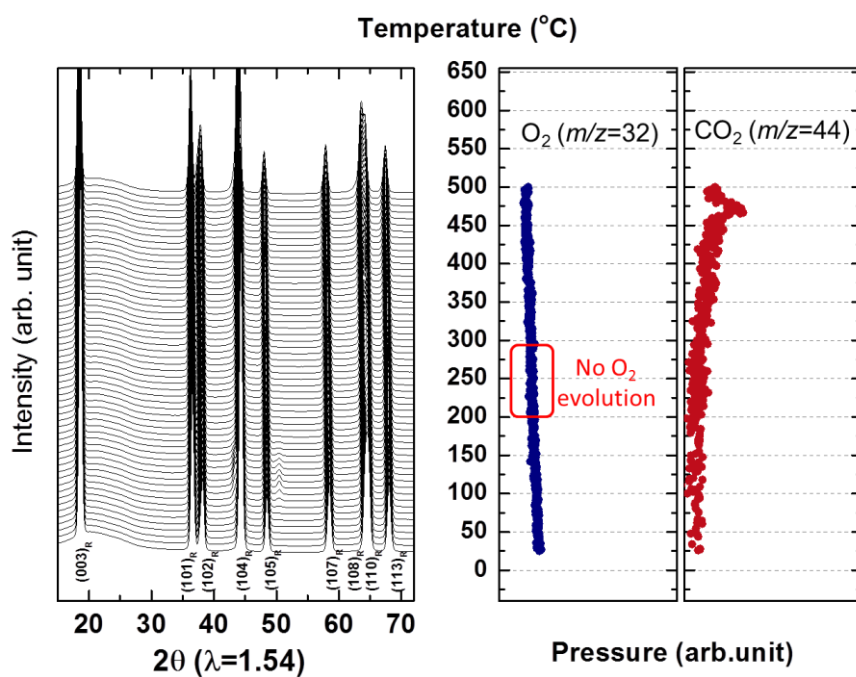


**Figure S3.** TR-XRD patterns and mass spectroscopy results for the pristine (uncharged)  $\text{LiNi}_{0.8}\text{Co}_{0.15}\text{Al}_{0.05}\text{O}_2$  after washing with DMC solvent.

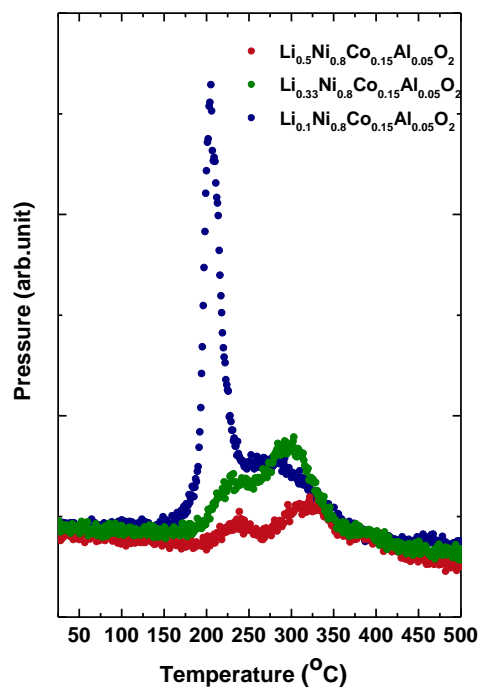


**Figure S4.** Mass spectroscopy (MS) results for O<sub>2</sub> release from  $\text{Li}_x\text{Ni}_{0.8}\text{Co}_{0.15}\text{Al}_{0.05}\text{O}_2$  (x=0.5, 0.33 and 0.1) during heating to 500°C.

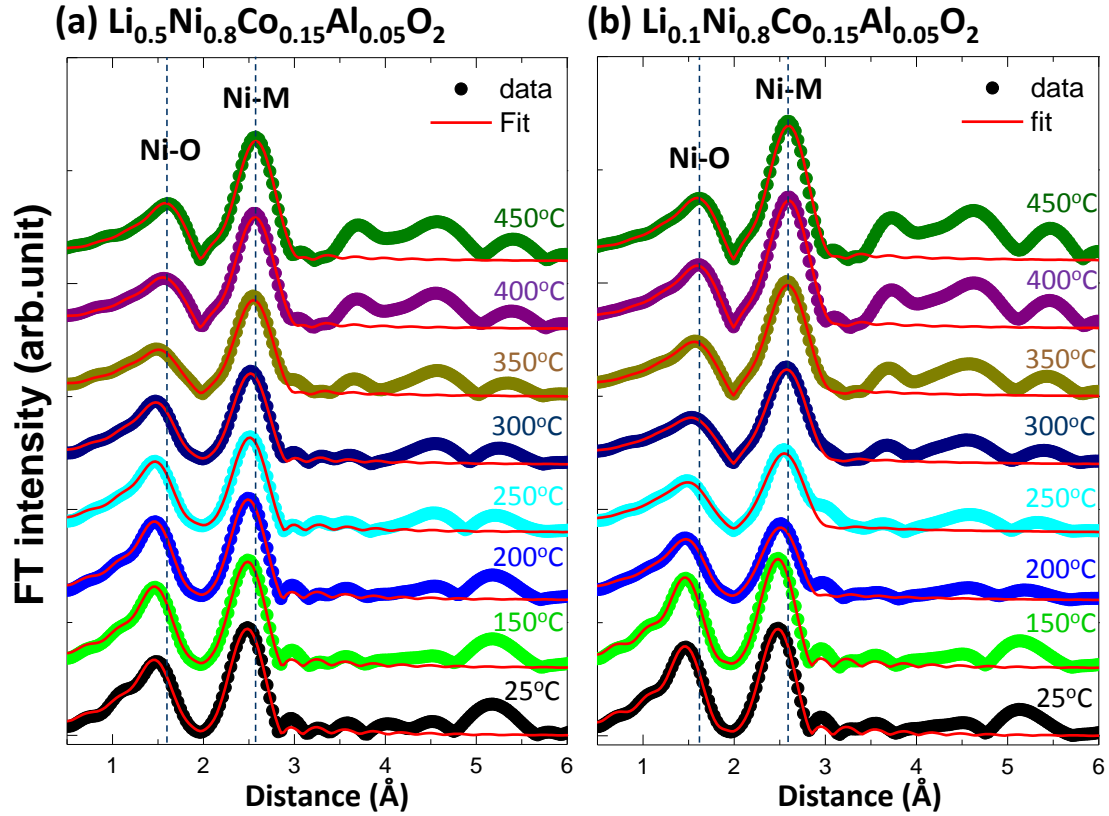


**Figure S5.** Experimental (solid circle) and fitted (red line) Fourier-transformed EXAFS spectra at Ni K-edge for the (a)  $\text{Li}_{0.5}\text{Ni}_{0.8}\text{Co}_{0.15}\text{Al}_{0.05}\text{O}_2$  and (b)  $\text{Li}_{0.1}\text{Ni}_{0.8}\text{Co}_{0.15}\text{Al}_{0.05}\text{O}_2$  with heating temperatures.

The EXAFS signal,  $\chi(k)$ , for the Ni K-edge was weighted by  $k^2$  to emphasize the high-energy oscillations and then Fourier-transformed in  $k$ -ranges of  $3.5 \sim 13.5 \text{ \AA}^{-1}$  using a Hanning window function ( $\Delta k = 1.0 \text{ \AA}^{-1}$ ) to obtain the magnitude plots of the EXAFS spectra in a  $R$ -space ( $\text{\AA}$ ). The filtered FTs of the EXAFS spectra in a  $R$  range of  $1.0 \sim 2.9 \text{ \AA}$  covering the first Ni-O and second Ni-M shells were fitted using theoretical single scattering paths generated with the FEFF 6.0 *ab-initio* simulation code based on a rock-salt model structure. The amplitude reduction factor ( $S_0^2$ ) was determined to be 0.75 from the preliminary fitting of the spectrum at 25°C (i.e., as charged samples) and then fixed during the final fitting unless noted otherwise. The same inner shell potential shift ( $\Delta E$ ) was shared for the Ni-O and Ni-M shells ( $M=\text{Co}$  and  $\text{Ni}$ ) while separate fitting parameters of the bond distance ( $R$ ) and Debye-Waller factor (i.e., mean square disorder,  $\sigma^2$ ) were used for each shell. The coordination number for the first Ni-O shell was fixed to 6 (i.e., octahedral coordination) while those of the second Ni-M shell were refined during fitting. Therefore total number of parameters varied during the fit was 6 which is far less than the number of independent parameters of around 12 which is given by the relation  $N_{\text{idp}} \approx (2\Delta k \Delta R)/\pi$  where  $\Delta R$  is the fitting range in  $R$  space and  $\Delta k$  is the data range in  $k$  space. The fitted  $\Delta E$  values for all of the Ni K-edge EXAFS spectra were between -5.0 and

0.0 which were acceptable. During the phase transition from ordered rock salt (i.e., layered structure) to disordered rock-salt (i.e., NaCl type rock salt structure) structure,  $S_0^2$  values needed to be adjusted from 0.75 to 0.98 since the fixed value of 0.75 resulted in the significant increase of the EXAFS reliability  $R$ -factor (i.e., absolute misfit between the data and fitting) for the spectra with high temperatures. Therefore, adjusted  $S_0^2$  value of 0.98 was used for the following Ni K-edge spectra;

- $\text{Li}_{0.5}\text{Ni}_{0.8}\text{Co}_{0.15}\text{Al}_{0.05}\text{O}_2$  spectra  $\geq 350^\circ\text{C}$
- $\text{Li}_{0.1}\text{Ni}_{0.8}\text{Co}_{0.15}\text{Al}_{0.05}\text{O}_2$  spectra  $\geq 250^\circ\text{C}$ .

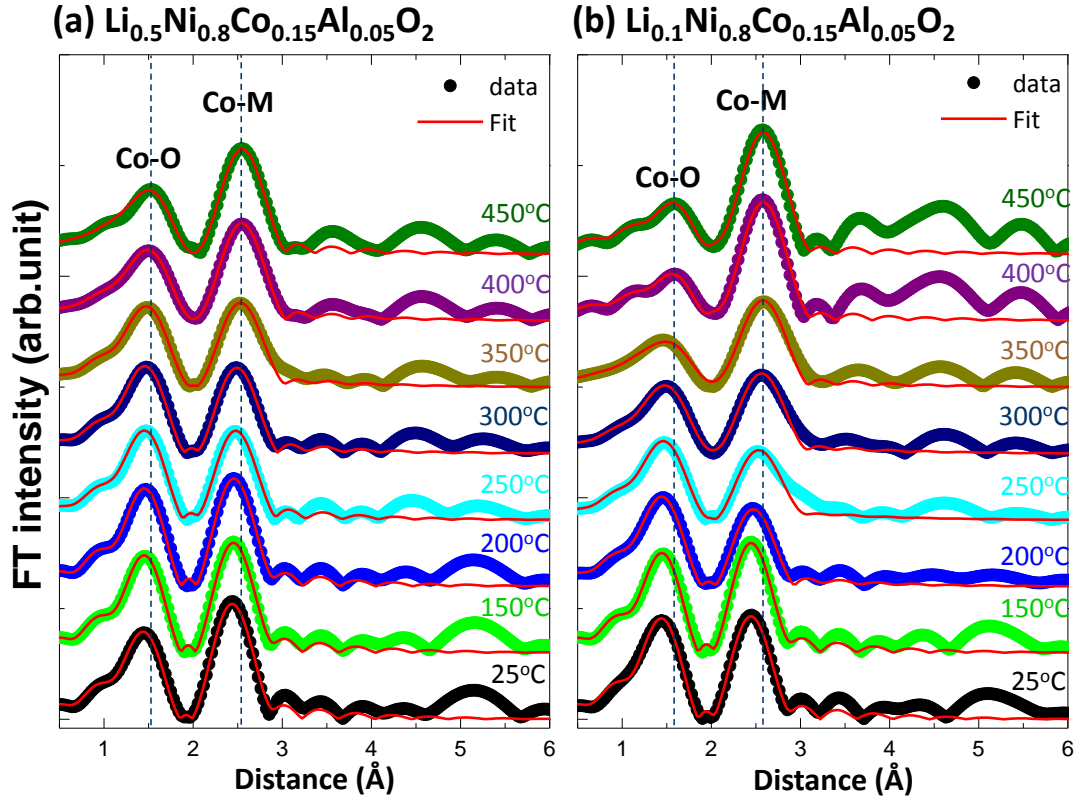


**Figure S6.** Fourier transformed experimental (solid circle) and fitted (red line) EXAFS data at Co K-edge for the (a)  $\text{Li}_{0.5}\text{Ni}_{0.8}\text{Co}_{0.15}\text{Al}_{0.05}\text{O}_2$  and (b)  $\text{Li}_{0.1}\text{Ni}_{0.8}\text{Co}_{0.15}\text{Al}_{0.05}\text{O}_2$  with heating temperatures.

The EXAFS signal,  $\chi(k)$ , for the Co K-edge was weighted by  $k^2$  to emphasize the high-energy oscillations and then Fourier-transformed in  $k$ -ranges of  $3.4 \sim 11.0 \text{ \AA}^{-1}$  using a Hanning window function ( $\Delta k = 1.0 \text{ \AA}^{-1}$ ) to obtain the magnitude plots of the EXAFS spectra in a R-space ( $\text{\AA}$ ). For the Co K-edge spectra,  $k$  range was limited to  $11.0 \text{ \AA}^{-1}$  due to the existence of Ni which appears at around  $12 \text{ \AA}^{-1}$  in the EXAFS signal,  $\chi(k)$ . The filtered FTs of the EXAFS spectra in a R range of  $1.0 \sim 2.9 \text{ \AA}$  covering the first Co-O and second Co-M shells were fitted using theoretical single scattering paths generated with the FEFF 6.0 *ab-initio* simulation code based on a rock-salt model structure. The amplitude reduction factor ( $S_0^2$ ) was determined to be 0.84 from the preliminary fitting of the spectrum at  $25^\circ\text{C}$  (i.e., as charged samples) and then fixed during the final fitting unless noted otherwise. The similar fitting scheme used for the Ni K-edge fitting was applied to the Co K-edge data for the inner shell potential shift ( $\Delta E$ ), bond distance ( $R$ ), Debye-Waller factor (i.e., mean square disorder,  $\sigma^2$ ), the coordination number. Total number of fitting parameters varied during the fit was 6 which is less than the number of independent parameters of around 9. The fitted  $\Delta E$  values for all of the Co K-edge EXAFS spectra were in the range of  $\pm 2.5$  which is acceptable. The  $S_0^2$  values were also adjusted from 0.84 to 0.95 in case of the Co K-edge spectra over  $350^\circ\text{C}$  for the highly charged

$\text{Li}_{0.1}\text{Ni}_{0.8}\text{Co}_{0.15}\text{Al}_{0.05}\text{O}_2$  sample while the  $S_0^2$  values for the spectra of the less charged  $\text{Li}_{0.5}\text{Ni}_{0.8}\text{Co}_{0.15}\text{Al}_{0.05}\text{O}_2$  samples were kept with the original value of 0.84.

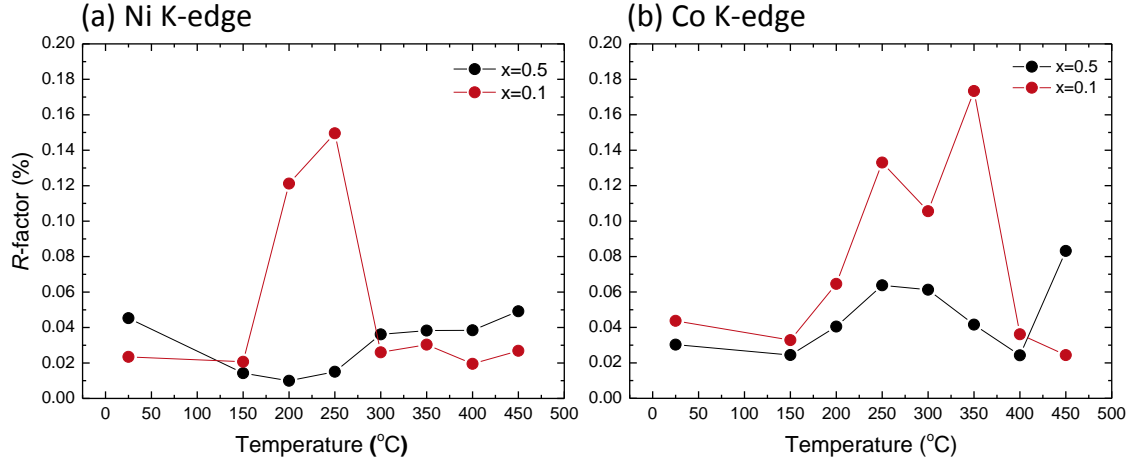


**Figure S7.** The EXAFS reliability  $R$ -factors for the fitting of Ni and Co K-edge EXAFS spectra of the charged  $\text{Li}_x\text{Ni}_{0.8}\text{Co}_{0.15}\text{Al}_{0.05}\text{O}_2$  with  $x=0.5$  and  $0.1$ .

The EXAFS reliability  $R$ -factor was estimated based on the following equation;

$$R = \sum_{i=1}^{N_{pts}} \frac{[Im(\chi_{dat}(R_i) - \chi_{th}(R_i))]^2 + [Re(\chi_{dat}(R_i) - \chi_{th}(R_i))]^2}{[Im(\chi_{dat}(R_i))]^2 + [Re(\chi_{dat}(R_i))]^2}$$

The EXAFS  $R$ -factors were less than 0.2% in all cases showing a good quality of the fitting based on the rock-salt model structure. However, compared with, the  $R$ -factors for the Co K-edge fitting (Fig. S7(b)) were relatively higher than those for the Ni K-edge fitting results (Fig. S7(a)) regardless of the states of charge. This may suggest that the formation of a different local structure (e.g.,  $\text{Co}_3\text{O}_4$  spinel) around Co, which is not a layered or rock-salt structure (only a rock-salt model was considered in the fitting). Alternative fittings of the Co and Ni K-edge EXAFS spectra for those which showed large misfit based on the rock-salt structure will be tested using different model structures such as spinel-  $\text{Co}_3\text{O}_4$  and  $\text{LiCo}_2\text{O}_4$  structures with some modifications (e.g., site occupancy and site mixing) in the future work.